

Developments of large eddy simulation for compressible space plasma turbulence

A.A. Chernyshov¹, K.V. Karelsky¹ and A.S. Petrosyan^{1,2}

¹ Theoretical section, Space Research Institute of Russian Academy of Sciences, 84/32 Profsoyuznaya, 117997, Moscow, Russia

² Moscow Institute of Physics and Technology (State University), 9 Institutskii per., 141700, Dolgoprudny, Moscow Region, Russia

E-mail: apetrosy@iki.rssi.ru

Abstract. In this paper, brief review of studies of compressible space plasma turbulence is given. Magnetic fields and compressibility are present that are different from properties of hydrodynamic incompressible turbulence of neutral fluid. This considerably complicates studies of characteristics of compressible magnetohydrodynamic turbulence with direct numerical simulation. Large eddy simulation method developed as alternative of direct modeling is discussed in the review. The method is based on filtering procedure of governing equations of magnetohydrodynamics and subgrid-scale modeling of universal small-scale turbulence. Descriptions of both the method and different subgrid-scale models for compressible magnetohydrodynamic turbulent flows are present. It is shown that large eddy simulation has good future trends for research of compressible magnetohydrodynamic turbulence.

1. Introduction

Numerical simulation of turbulent magnetohydrodynamic (MHD) flows is an effective tool for the study of the flows of the charged fluid of astrophysical, helio- and geophysical plasma (for instance, solar corona expansion, solar wind, flows in the solar convection zone, turbulence in interstellar matter), that is beyond the reach of direct experimental study. Besides, MHD turbulence are widely encountered in various applied areas, for example, it is possible to mention actual studies of the noise decrease, using plasma actuator for control of large vortex structures in jets, investigations of decrease of turbulent flow resistance in aerospace industry, MHD flow in a channel for steel-casting process and in pipe for cooling of nuclear fusion reactors.

Complete information about turbulent fluid flow could be obtained by means of direct numerical simulation (DNS) that is in the numerical solution of full nonstationary system of magnetohydrodynamic equations. This approach allows resolving all scales of charged fluid flows and does not require special closures for magnetohydrodynamic equations. However, direct numerical computation of MHD-turbulence faces fundamental difficulties related to the large hydrodynamic and magnetic Reynolds numbers typical for studied processes. In that case the number of degrees of freedom of turbulent flow is large and minimal number of mesh points must be so large that application of direct numerical simulation for study of turbulent flows with real Reynolds numbers is limited by available computational resources.

Large eddy simulation (LES) approach describes approximate turbulence dynamics, where the large-scale part of turbulent flow is computed directly, while the small-scale one is modeled.



Possibility of using filtration operation in LES for decomposition of turbulent flow characteristics into large-scale and small-scale parts is due to sufficient isotropy, homogeneity and universality of small scales of turbulent flow. Under these conditions small-scale flow is eliminated from the initial system of flow equations with the use of filtration procedure and then their influence is taken into account by means of subgrid-scale (SGS) models (otherwise called by subfilter scale (SFS)), parameterizing all the magnetohydrodynamic values of small-scale turbulent flow through the filtered ones. Thus, large-scale motion is computed by means of solving of the filtered non-stationary equations of magnetohydrodynamics. LES is a method for simulation of flows with large Reynolds numbers, since LES assumes that the energy is transferred within the inertial subrange that results in reduction of number of degrees of freedom and significant increase of computation efficiency as compared with DNS.

Recently, LES approach for study of compressible forced and decaying MHD turbulence has been developed for the cases of polytropic gas and heat-conducting plasma [1, 2, 3, 4, 5, 6, 3, 7, 8, 9]. This paper is a review latest achievements in the development of LES method of compressible MHD turbulence. Here we restrict ourselves to the case of MHD turbulence of polytropic fluid. In this review, we briefly describe the basic concepts and principles of LES, the subgrid-scale modeling, dynamic procedure in MHD and the important results and conclusions.

2. Governing equations and Subgrid-scale models

In this section, we formulate the theory of large eddy simulation for compressible magnetohydrodynamics and obtain filtered MHD equations. Subgrid scale modeling in LES is discussed and various closure models for compressible MHD case are proposed.

To obtain the MHD equations governing the motion of the filtered (that is resolved) eddies, the large scales from the small are separated. LES approach is based on the definition of a filtering operation: a resolved (or large-scale) variable, denoted by an overbar in the present paper, is defined as

$$\bar{f}(x_i) = \int_{\Theta} f(x'_i) G(x_i, x'_i; \bar{\Delta}) dx'_i, \quad (1)$$

where G is the filter function satisfying the normalization property, Θ is the domain, $\bar{\Delta}$ is the filter-width associated with the wavelength of the smallest scale retained by the filtering procedure and $x_j = (x, y, z)$ are axes of Cartesian coordinate system.

It is convenient to use the Favre filtration (it is also called mass-weighted filtration) to avoid additional SGS terms in compressible flow. Therefore, Favre filtering will be used further on. Mass-weighted filtering is determined as follows: $\tilde{f} = \bar{\rho} f / \bar{\rho}$, where the tilde denotes the mass-weighted filtration.

Thus, applying the Favre-filtering operation, we can rewrite the MHD equations for compressible fluid flow as:

$$\frac{\partial \bar{\rho}}{\partial t} + \frac{\partial \bar{\rho} \tilde{u}_j}{\partial x_j} = 0; \quad (2)$$

$$\frac{\partial \bar{\rho} \tilde{u}_i}{\partial t} + \frac{\partial}{\partial x_j} \left(\bar{\rho} \tilde{u}_i \tilde{u}_j + \frac{\bar{\rho} \gamma}{\gamma M_s^2} \delta_{ij} - \frac{1}{Re} \sigma_{ij} + \frac{\bar{B}^2}{2M_a^2} \delta_{ij} - \frac{1}{M_a^2} \bar{B}_j \bar{B}_i \right) = - \frac{\partial \tau_{ji}^u}{\partial x_j}; \quad (3)$$

$$\frac{\partial \bar{B}_i}{\partial t} + \frac{\partial}{\partial x_j} (\tilde{u}_j \bar{B}_i - \tilde{u}_i \bar{B}_j) - \frac{1}{Re_m} \frac{\partial^2 \bar{B}_i}{\partial x_j^2} = - \frac{\partial \tau_{ji}^b}{\partial x_j}; \quad (4)$$

$$\frac{\partial \bar{B}_j}{\partial x_j} = 0, \quad (5)$$

Here ρ is the density; u_j is the velocity in the direction x_j ; B_j is the magnetic field in the direction x_j ; $\sigma_{ij} = 2\mu S_{ij} - \frac{2}{3}\mu S_{kk}\delta_{ij}$ is the viscous stress tensor; $S_{ij} = 1/2 (\partial u_i / \partial x_j + \partial u_j / \partial x_i)$

is the strain rate tensor; μ is the coefficient of molecular viscosity; η is the coefficient of magnetic diffusivity; δ_{ij} is the Kronecker delta.

The filtered magnetohydrodynamic equations (2) - (5) are written in the dimensionless form using the standard procedure [10] where $Re = \rho_0 u_0 L_0 / \mu_0$ is the Reynolds number, $Re_m = u_0 L_0 / \eta_0$ is the magnetic Reynolds number. $M_s = u_0 / c_s$ is the Mach number, where c_s is the velocity of sound defined by the relation $c_s = \sqrt{\gamma p_0 / \rho_0}$, and $M_a = u_0 / u_a$ is the magnetic Mach number, where $u_a = B_0 / (\sqrt{4\pi\rho_0})$ is the Alfvén velocity.

To close the equations (2) - (4) it is assumed that the relation between density and pressure is polytropic and has the following form: $p = \rho^\gamma$, where γ is a polytropic index and it is supposed that $\gamma = 5/3$.

The effect of the SGSs appears on the right-hand side of the governing equations (3) - (4) through the SGS stresses:

$$\tau_{ij}^u = \bar{\rho} (\widetilde{u_i u_j} - \tilde{u}_i \tilde{u}_j) - \frac{1}{M_a^2} (\overline{B_i B_j} - \bar{B}_i \bar{B}_j); \quad (6)$$

$$\tau_{ij}^b = (\overline{u_i B_j} - \tilde{u}_i \bar{B}_j) - (\overline{B_i u_j} - \bar{B}_i \tilde{u}_j). \quad (7)$$

Consequently, the filtered system of magnetohydrodynamic equations contains the unknown turbulent tensors: τ_{ij}^u and τ_{ij}^b . To determine their components special turbulent closures (models, parameterizations) based on large-scale values describing turbulent magnetohydrodynamic flow must be used. The main idea of any SGS closures used in LES is to reproduce the effects of the subgrid scale dynamics on the large-scale energy distribution, at that as a matter of fact Richardson turbulent cascade is simulated. In order to close the system of MHD equations we should find such parameterizations for τ_{ij}^u and τ_{ij}^b that would relate these tensors to the known large-scale values of the flow parameters.

In this paper we consider five SGS models and three of them (the Smagorinsky model for MHD case, Kolmogorov model for MHD-turbulence, model based on cross-helicity) use eddy-viscosity assumption to try to simulate the diffusive transport and dissipation of kinetic and magnetic energy. One of them (scale-similar model) is based on the assumption that the most active SGSs are those closer to the cutoff, and that the scales with which they interact are those immediately above the cutoff wave number. Also, the last SGS closures considered in present work is mixed model for MHD turbulence.

The first model is the Smagorinsky model. In [4], we represent its extension to the MHD-case for compressible turbulence, given by

$$\tau_{ij}^u - \frac{1}{3} \tau_{kk}^u \delta_{ij} = -2C_1 \bar{\rho} \bar{\Delta}^2 |\tilde{S}^u| \left(\tilde{S}_{ij} - \frac{1}{3} \tilde{S}_{kk} \delta_{ij} \right), \quad (8)$$

$$\tau_{ij}^b = -2D_1 \bar{\Delta}^2 |\bar{j}| \bar{J}_{ij}, \quad (9)$$

$$\tau_{kk}^u = 2Y_1 \bar{\rho} \bar{\Delta}^2 |\tilde{S}^u|^2 \quad (10)$$

where \bar{j} is the resolved electric current density, $\tilde{S}_{ij} = (\partial \tilde{u}_i / \partial x_j + \partial \tilde{u}_j / \partial x_i) / 2$ is a large-scale strain rate tensor, $\bar{J}_{ij} = (\partial \bar{B}_i / \partial x_j - \partial \bar{B}_j / \partial x_i) / 2$ is a large-scale magnetic rotation tensor and $|\tilde{S}^u| = \left(2 \tilde{S}_{ij}^u \tilde{S}_{ij}^u \right)^{1/2}$.

The generalized Kolmogorov scaling subgrid model for MHD compressible turbulence is

$$\tau_{ij}^u - \frac{1}{3} \tau_{kk}^u \delta_{ij} = -2C_2 \bar{\rho} \bar{\Delta}^{4/3} \left(\tilde{S}_{ij} - \frac{1}{3} \tilde{S}_{kk} \delta_{ij} \right), \quad (11)$$

$$\tau_{ij}^b = -2D_2 \bar{\Delta}^{4/3} \bar{J}_{ij}, \quad (12)$$

$$\tau_{kk}^u = 2Y_2\bar{\rho}\bar{\Delta}^{4/3}|\tilde{S}^u| \quad (13)$$

The third model examined in this paper uses the local cross-helicity change instead of the energy dissipation functions. Therefore, the model based on cross-helicity is defined as:

$$\tau_{ij}^u - \frac{1}{3}\tau_{kk}^u\delta_{ij} = -2C_3\bar{\rho}\bar{\Delta}^2|\tilde{f}|\left(\tilde{S}_{ij} - \frac{1}{3}\tilde{S}_{kk}\delta_{ij}\right), \quad (14)$$

$$\tau_{ij}^b = -2D_3\bar{\Delta}^2\text{sgn}(\bar{j}\tilde{\omega})|\bar{j}\tilde{\omega}|^{1/2}\bar{J}_{ij}, \quad (15)$$

$$\tau_{kk}^u = 2Y_3\bar{\rho}\bar{\Delta}^2|\tilde{f}||\tilde{S}^u| \quad (16)$$

Here, $\bar{S}_{ij}^b = (\partial\bar{B}_i/\partial x_j + \partial\bar{B}_j/\partial x_i)/2$, $\tilde{S}_{ij} = (\partial\tilde{u}_i/\partial x_j + \partial\tilde{u}_j/\partial x_i)/2$, $\tilde{f} = |\tilde{S}_{ij} \bar{S}_{ij}^b|^{1/2}$, $\tilde{\omega} = \nabla \times \tilde{u}$ is the vorticity and function $\text{sgn}(\cdot)$ determines the sign of the argument.

The scale-similarity model can be calculated in a LES by means of the filtered variables in contrast to other models. In a priori tests, the scale-similarity model reproduces the correlation between this model and actual turbulent stress tensor very well even when the flow is highly anisotropic [11]. This indicate that the similarity model predicts important structures of the turbulent stress at the right locations. One of the main advantages of the scale-similarity model is that it does not require a determination of special model constants in contrast to the eddy-viscosity parameterizations. The scale-similarity model are based on the assumption that the most active subgrid scales are those closer to the cutoff wave number, and that the scales with which they interact most are those right above the cutoff [12]. The "largest subgrid scales" can be obtained by filtering the SGS parameter, for example, velocity $\tilde{u}_j = u_j - \tilde{u}_j$ to yield $\tilde{\tilde{u}}_j = \tilde{u}_j - \tilde{\tilde{u}}_j$. The scale-similarity model for MHD compressible case is written in the following manner:

$$\tau_{ij}^u = \bar{\rho}\left(\widetilde{\tilde{u}_i\tilde{u}_j} - \tilde{\tilde{u}}_i\tilde{\tilde{u}}_j\right) - \frac{1}{M_a^2}\left(\overline{\tilde{B}_i\tilde{B}_j} - \bar{\tilde{B}}_i\bar{\tilde{B}}_j\right) \quad (17)$$

$$\tau_{ij}^b = \left(\overline{\tilde{u}_i\tilde{B}_j} - \tilde{\tilde{u}}_i\bar{\tilde{B}}_j\right) - \left(\overline{\tilde{B}_i\tilde{u}_j} - \bar{\tilde{B}}_i\tilde{\tilde{u}}_j\right) \quad (18)$$

The mixed model for MHD compressible turbulence is a combination of two models: the scale similarity and the Smagorinsky models for MHD case:

$$\tau_{ij}^u - \frac{1}{3}\tau_{kk}^u\delta_{ij} = -2C_5\bar{\rho}\bar{\Delta}^2|\tilde{S}^u|\left(\tilde{S}_{ij} - \frac{\delta_{ij}}{3}\tilde{S}_{kk}\right) + \bar{\rho}\left(\widetilde{\tilde{u}_i\tilde{u}_j} - \tilde{\tilde{u}}_i\tilde{\tilde{u}}_j\right) - \frac{1}{M_a^2}\left(\overline{\tilde{B}_i\tilde{B}_j} - \bar{\tilde{B}}_i\bar{\tilde{B}}_j\right) \quad (19)$$

$$\tau_{ij}^b = -2D_5\bar{\Delta}^2|\bar{j}|\bar{J}_{ij} + \left(\overline{\tilde{u}_i\tilde{B}_j} - \tilde{\tilde{u}}_i\bar{\tilde{B}}_j\right) - \left(\overline{\tilde{B}_i\tilde{u}_j} - \bar{\tilde{B}}_i\tilde{\tilde{u}}_j\right) \quad (20)$$

$$\tau_{kk}^u = 2Y_5\bar{\rho}\bar{\Delta}^2|\tilde{S}^u|^2 \quad (21)$$

The parameters C_k , Y_k and D_k ($k = 1, 2, 3$ or 5) are model constants, their values being self-consistently computed during run time with the help of the dynamic procedure that explains in next section.

3. Dynamic procedure in MHD

In order to solve the problem concerning the choice of the constants, Germano suggested a dynamic procedure [13, 14] that determines the value of the constant at every time step. Then, this technique for determination of model constants has been applied for incompressible [15] and compressible MHD turbulence [1].

In this method an additional test filter with width more than the width of the basic one is used. Let T_{ij}^u and T_{ij}^b obtained with use of test filter be the test subgrid tensors for τ_{ij}^u and τ_{ij}^b , respectively.

$$T_{ij}^u = \tilde{\tilde{\tau}}_{ij}^u + L_{ij}^u, \quad (22)$$

$$T_{ij}^b = \bar{\tau}_{ij}^b + L_{ij}^b, \quad (23)$$

where Leonard tensors:

$$L_{ij}^u = \left(\frac{\widehat{\rho u_i \rho u_j}}{\bar{\rho}} \right) - \frac{\widehat{\rho u_i} \widehat{\rho u_j}}{\hat{\rho}} - \frac{1}{M_a^2} \left(\widehat{\bar{B}_i \bar{B}_j} - \hat{\bar{B}}_i \hat{\bar{B}}_j \right), \quad (24)$$

$$L_{ij}^b = \left(\left(\frac{\widehat{\rho u_i} \bar{B}_j}{\bar{\rho}} \right) - \frac{\widehat{\rho u_i} \widehat{\bar{B}}_j}{\hat{\rho}} \right) - \left(\left(\frac{\widehat{\bar{B}_i} \rho u_j}{\bar{\rho}} \right) - \frac{\widehat{\bar{B}_i} \widehat{\rho u_j}}{\hat{\rho}} \right). \quad (25)$$

Here, the sign $\hat{\cdot}$ designates a test filtration of variable. The Leonard tensors L_{ij}^u and L_{ij}^b can be found from the large-scale values of velocity and magnetic field. The relations (24) and (25) connect initial subgrid and test tensors.

Let us define the turbulent viscosity and magnetic diffusion coefficients as follows: $\nu_t = C_s \alpha_{ij}^u$ (for τ_{ij}^u), $\dot{\nu}_t = C_I \alpha^u$ (for τ_{kk}^u), $\eta_t = D \varphi_{ij}^B$ (for τ_{ij}^b).

The least-squares method for determination of the constants to minimize errors of functionals is applied [16]:

$$Z^u = \langle (T_{ij}^u - \hat{\tau}_{ij}^u - L_{ij}^u)^2 \rangle, \quad (26)$$

$$Z^b = \langle (T_{ij}^b - \hat{\tau}_{ij}^b - L_{ij}^b)^2 \rangle. \quad (27)$$

where the angle brackets denote spatial averaging.

Consequently, the constants are determined dynamically at every time step according to the following expressions:

$$C_s = \frac{\langle L_{ij}^u M_{ij}^u \rangle}{\langle M_{ij}^u M_{ij}^u \rangle}, \quad (28)$$

$$C_I = \frac{\langle L_{kk}^u \rangle}{\langle \hat{\alpha}^u |\hat{S}^u| - \alpha^u |S^u| \rangle}, \quad (29)$$

$$D = \frac{\langle L_{ij}^b m_{ij}^B \rangle}{\langle m_{ij}^B m_{lk}^B \rangle}, \quad (30)$$

where

$$M_{ij}^u = \hat{\alpha}_{ij}^u \left(\hat{S}_{ij}^u - \frac{\delta_{ij}}{3} \hat{S}_{kk}^u \right) - \left[\alpha_{ij}^u \left(\tilde{S}_{ij}^u - \frac{\delta_{ij}}{3} \tilde{S}_{kk}^u \right) \right]^{\hat{\cdot}}, \quad (31)$$

$$m_{ij}^B = \hat{\varphi}_B \hat{J}_{ij} - \widehat{\varphi_B J_{ij}}. \quad (32)$$

Here $[\cdot]^{\hat{\cdot}}$ indicates that test filtering procedure applies to the expression in square brackets. It should be noted, that the Favre-filtered task variables in the initial equations also have to be Favre-filtered in case of use of test filter. Here, denotation \hat{u} signifies $\hat{u} = \widehat{\rho u} / \hat{\rho}$. The characteristic width of the test filter as a rule is usually taken twice more, i.e. $\hat{\Delta} = 2\bar{\Delta}$.

It is important to note, that the values of constants can be negative that correspond to energy backscatter, i.e. to the local gain of energy at the resolved scales.

4. Aspects of numerics

In our works, numerical code of the fourth order of accuracy for MHD equations written in the conservative form is used. The skew-symmetric form is applied for the nonlinear terms, because the skew-symmetric form of the equation is a form obtained by averaging divergence form and convective form of the nonlinear term. In spite of analytical equivalence of all the three of these forms, their numerical computations give different results. To reduce error of discretization when finite difference scheme is used and to improve computational accuracy the skew-symmetric discretization is applied for nonlinear terms. For numerical solution of system of MHD equations, in this work we use the numerical code based on non-spectral finite-difference schemes. To separate the turbulent flow into large and small eddy components, discrete Gaussian filter of the fourth order of accuracy is applied.

For the performance evaluation of various subgrid-scale closures in the LES approach, direct numerical simulation results obtained by modeling of MHD turbulence over a various range of magnetic Reynolds number, hydrodynamic Reynolds number and Mach number are presented in detail in [4]. DNS calculations are performed on a sufficient grid size so that the accuracy of the obtained results provide real dynamics of three-dimensional compressible MHD turbulence and allow comparison with LES calculations. Initial data for all numerical calculations were chosen so that to provide a regime of developed turbulence and express the role of magnetic effects in MHD flow (see paper [4] for detailed information).

The results obtained by large eddy simulation are compared with DNS computations and performance of large eddy simulation is examined by difference between LES- and filtered DNS-results. The initial conditions for LES are obtained by filtering the initial conditions of DNS. The initial velocities and magnetic fields are chosen to resemble a MHD mixing layer by adapting the hydrodynamic case for study of decaying turbulence. The shear for velocity and magnetic field in the initial conditions is given z - coordinate depending [4]. The Courant-Friedrichs-Levy stability condition (CFL-condition) is imposed on the time step. The uniform mesh with 64^3 grid cells is used for LES and 256^3 for DNS. For time integration the third order low-storage Runge-Kutta method is used. Periodic boundary conditions for all the three dimensions are applied, the simulation domain is a cube with dimensions of $2\pi \times 2\pi \times 2\pi$. The model constants in subgrid-scale closures are determined by means of the dynamic procedure and test filter with filter width twice as large as initial one is used.

For the case of forced MHD turbulence, the initial isotropic turbulent spectrum close to k^{-2} with random amplitudes and phases in all three directions was chosen for kinetic and magnetic energies in Fourier space. The choice of such spectrum as initial conditions is due to velocity perturbations with an initial power spectrum in Fourier space similar to that of developed turbulence [17]. This k^{-2} spectrum corresponds to spectrum of Burgers turbulence. Initial conditions for the velocity and the magnetic field have been obtained in the physical space using inverse Fourier transform. In this case, the simulation domain is a cube $\pi \times \pi \times \pi$.

5. LES of decaying compressible MHD turbulence

We perform three-dimensional numerical simulation of decaying compressible MHD turbulence. For the performance evaluation of various subgrid-scale closures in the LES approach, direct numerical simulation results obtained by modeling of MHD turbulence over a various range of magnetic Reynolds number, hydrodynamic Reynolds number and Mach number are presented in this survey. DNS calculations are performed on a sufficient grid size so that the accuracy of the obtained results provide real dynamics of three-dimensional compressible MHD turbulence and allow comparison with LES calculations.

Time dynamics of the kinetic and magnetic energy respectively are displayed in Fig. 1 and Fig. 2. Fig3 shows time evolution of the cross-helicity. The computation results are presented for the following initial parameters of compressible MHD turbulence: $\lambda = 0, 84$ is Taylor microscale,

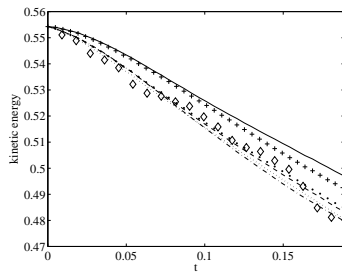


Figure 1. Time evolution of the kinetic energy.

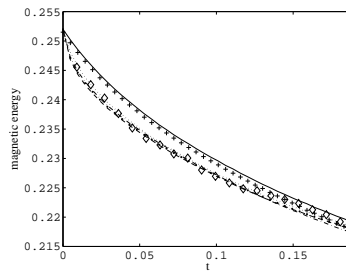


Figure 2. Time evolution of the magnetic energy.

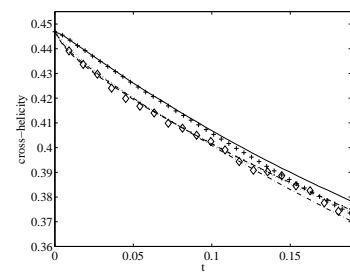


Figure 3. Time dynamics of the cross-helicity.

$Re = 390$ is hydrodynamic Reynolds number, $Re_m = 10$ is magnetic Reynolds number, $M_s = 0.6$ is Mach number, $\kappa = 0.8$ is Kolmogorov scale, $\mu = 0.01$ is coefficient of molecular viscosity and $\gamma = 5/3$ is polytropic index. The solid line corresponds to the case when tensors τ_{ij}^u and τ_{ij}^b are omitted, which means that LES, in fact, is DNS on the coarse LES-grid starting from filtered initial conditions. The solid line is included here for a more detailed analysis and understanding of an influence SGS models on the modeling of MHD flow for comparison DNS results with LES results made by various SGS models. The dashed line denotes the Smagorinsky model for MHD-turbulence, the dotted line is the Kolmogorov model, the black point line is the model based on cross-helicity. The marker + is the scale-similarity model and the dashed-dot line represents the mixed model for MHD-case. The DNS results are represented by the diamond line. As expected, the results of model without subgrid parametrization exhibit the largest deviation from DNS results. It follows from Fig. 1 and Fig. 2, that the similarity model gives the worst predictions among SGS closures. The other subgrid models significantly improve the calculation accuracy.

The differences between SGS models for magnetic energy are shown to decrease with reducing magnetic Reynolds number and all models discussed above demonstrate good agreement with DNS results at small magnetic Reynolds number. The effect of subgrid-scale closures increases with magnetic Reynolds number for modeling of compressible MHD turbulence, but rate of dissipation of the magnetic energy decreases with increasing magnetic Reynolds number. The best results are shown for the Smagorinsky, the Kolmogorov and the cross-helicity models for evolution of the magnetic energy. The same behaviour of plots was observed for the cross-helicity: the influence of subgrid-scale parameterizations increases with magnetic Reynolds number.

For kinetic energy larger divergence of LES results is observed with decrease in magnetic Reynolds number using various SGS closures. The scale-similarity model shows the worst results, however, the other SGS closures increase calculation accuracy. For time dynamics of both magnetic turbulent intensities and kinetic turbulent intensities, the impact of SGS parameterizations on results of modeling of MHD flow increase with magnetic Reynolds number. The role of anisotropy in computations and the divergences between LES and DNS results for anisotropy increase with decreasing magnetic Reynolds number.

Sonic Mach number exerts essential influence on results of modeling [4]. The divergence between DNS and LES results for kinetic energy increases with Mach number. The Smagorinsky model and the cross-helicity model yield the best accordance with DNS under various Mach number. The deviations in results for magnetic energy, on the contrary, decrease with increasing Mach number. It is necessary to notice, that magnetic energy reaches a stationary level more rapidly with reducing Mach number. The Smagorinsky model shows the best results for cross-helicity both for high and for low Mach numbers. The skewness of velocity components, calculated with the use of LES, coincides better with DNS results with increasing Mach number. The choice of SGS parametrization virtually did not have an effect on skewness of magnetic field

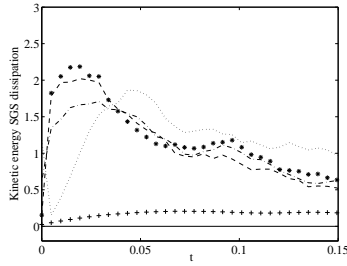


Figure 4. Time evolution of the kinetic energy subgrid dissipation.

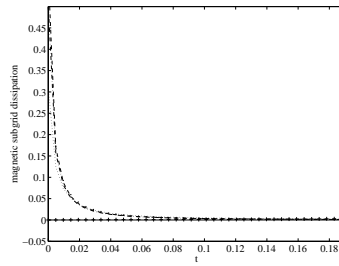


Figure 5. Time evolution of the magnetic energy subgrid dissipation.

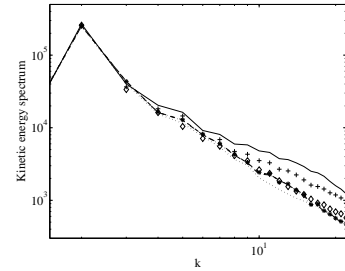


Figure 6. Kinetic energy spectrum.

components. The turbulent intensities obtained by LES technique agree better with DNS results with increasing Mach number.

Time evolution of the kinetic energy subgrid scale dissipation is plotted in Fig. 4. Here notations are the same as in the Fig. 10-Fig. 3 but the black point line is the model based on cross-helicity. This term, defined here as $\chi_u = -\tau_{ij}^u \tilde{S}_{ij}$, is written so that to be a sink of filtered kinetic energy when $\chi_u > 0$ and a source when $\chi_u < 0$ (i.e., backscatter). The value χ_u defines the amount of energy which transfers from large scale to subgrid scale and χ_u depends from SGS models that is used to find the subgrid tensor τ_{ij}^u . It is clear that SGS dissipation for scale-similarity model till the time $t = 0.13$ is the minimum, therefore this SGS model does not supply with the dissipation of kinetic energy properly and in Fig. 1 scale-similarity model demonstrates the worst results. The most value of the subgrid dissipation of kinetic energy is available for Kolmogorov and mixed models. The magnetic energy subgrid scale dissipation is determined as $\chi_b = -\tau_{ij}^b \tilde{J}_{ij}$, and represents the large-scale energy drained by the subgrid scales, forward scatter corresponds to $\chi_b > 0$ and backscatter to $\chi_b < 0$ (see Fig. 5). Magnetic subgrid energy is much less for scale-similarity closure, than for other SGS models [4].

One more test for the LES provides the spectral distribution of the kinetic and the magnetic energies that shows redistribution of energy depending on wavenumber, i.e. at different scales. Besides that, spectrum allows to estimate influence of subgrid closure models on properties of compressible turbulent flow. The Fig. 6 and Fig. 7 present curves for kinetic and magnetic energy spectra respectively (k is the wavenumber). It is clear that at large scales (small values of wavenumber) plots of curves practically coincide, and the dependence from subgrid parameterizations virtually disappears. The largest scales are mostly independent of the applied subgrid-scale modeling approach. The distinction become apparent mainly at small scales (corresponding to large wave numbers). In general, the study of the energy spectra confirm the observations of the subgrid model performances made earlier. The spectrum of the filtered DNS is in good agreement with the Smagorinsky, Kolmogorov, cross-helicity and mixed models, with a slight preference for cross-helicity model and mixed model. Moreover, we observe that the simulations with the scale-similarity closure and no SGS model are not able to generate the requisite amount of the dissipation, in other words, these cases exhibit a energy pile-up due to the lack of dissipation and the contributions of high wavenumber are too high. These outcomes confirm the results obtained from the time evolution of the kinetic and magnetic energy [5, 1].

Interesting and important results were obtained in [7] where validation of LES method for study of flatness (or kurtosis) and skewness of decaying compressible magnetohydrodynamic turbulence was investigated. The skewness and the kurtosis of a velocity component are, respectively, defined as:

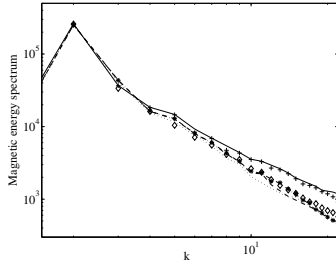


Figure 7. Magnetic energy spectrum.

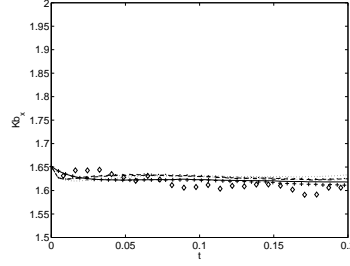


Figure 8. Time dynamics of flatness of the magnetic field

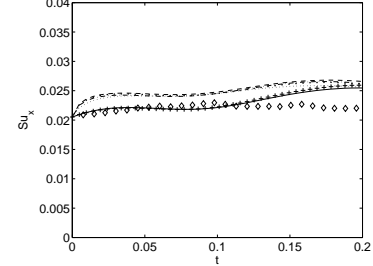


Figure 9. Time dynamics of skewness of the velocity

$$Su_j = \frac{\langle u_j^3 \rangle}{(\langle u_j^2 \rangle)^{3/2}} \quad Ku_j = \frac{\langle u_j^4 \rangle}{(\langle u_j^2 \rangle)^2} \quad (33)$$

The sample of comparison of various subgrid-scale models of LES and DNS for flatness of the magnetic field Kb_x and for skewness of the velocity Su_x is represented in Fig. 8 and Fig. 9, respectively. The flatness and the skewness define properties of probability density for the turbulent process. It is shown that the subgrid-scale parametrization choice for the flatness and the skewness of the velocity is more essential than for the same characteristics of the magnetic field. In consequence of the investigation carried out, it is shown that LES method provides adequate results and LES technique may be used for studying of PDF characteristics (for instance, structural functions of various moments of velocity and magnetic field) of compressible MHD fluid flow at various similarity numbers [7].

6. LES of forced compressible MHD turbulence

Magnetohydrodynamic turbulence, similar to hydrodynamic turbulence, possesses scale-similarity properties in the inertial range. A fully developed turbulent state is expected when the integral and dissipation scales are separated by several orders of magnitude.

Validity of the LES method for studies of physical processes in forced compressible MHD turbulence until recently remained unidentified. The problem is that in the case of compressible MHD turbulence for numerical solutions of filtered equations in LES (as well as for the solutions of governing equations in the DNS approach) the finite-difference and finite-volume schemes in coordinate (or physical) space are the most proper. Moreover, the solutions of the basic equations by finite-difference methods allow to investigate inhomogeneous and non-stationary turbulent flows directly. The traditional way of driving force implementation for the compressible MHD flows relies on studies of incompressible turbulent fluid and is based on the spectral representation of the external force and a subsequent re-calculation of this force in physical space. It should be noted that in compressible MHD there are four types of waves: Alfven, fast magnetosonic, slow magnetosonic and entropy. In this case the interactions between the aforementioned types of waves can lead to the richer picture of the turbulence spectra in the inertial range. The traditional forms of external forces (based on local spectral representations of a turbulence source) can strongly oversimplify the flow pattern in compressible MHD turbulence and so simplify the description of such turbulence under various similarity parameters. In this case the validation of the LES method requires proving the possibility of reproducing of the scale-similarity Kolmogorov and Iroshnikov-Kraichnan spectra in natural conditions. The work [9] is devoted to study of this important aspect of the LES method.

For the study of forced compressible MHD turbulence in the inertial range we apply the

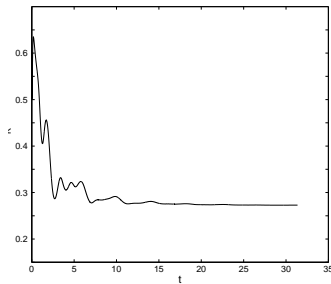


Figure 10. Time evolution of the kinetic energy with linear forcing.

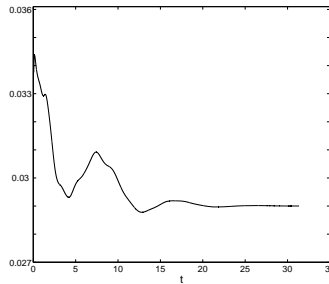


Figure 11. Time evolution of the magnetic energy with linear forcing.

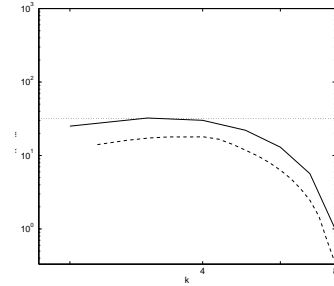


Figure 12. Normalized spectra of kinetic energy (solid line) and magnetic energy (dashed line).

linear driving force [9, 8]. The idea of linear forcing is to add a force proportional to the fluctuating velocity that resembles a turbulence which forced with a mean velocity gradient, that is, a shear. This force appears as a term in the equation for the fluctuating velocity that corresponds to the production term in the equation of turbulent kinetic energy. In this work, we generalize this approach to the case of compressible MHD flow of electrically conductive fluid. Such approach is called "linear forcing". Since compressible MHD turbulence is considered, the system of MHD equations includes the magnetic induction equation, and in this case the driving force is proportional to the magnetic field in the induction equation. In contrast to a spectral representation of the external force, the linear driving force acts on all scales of the physical space, and thereby it can reproduce more precisely a picture of mode interactions in compressible turbulent MHD flow. Actually, linear forcing corresponds to a turbulence with the driving force being caused by a mean velocity gradient, that is, by velocity shear. In the magnetic induction equation, the linear external force can be interpreted as being responsible for the production of magnetic energy due to the interaction between the magnetic field and the mean flow-velocity shear. In the works [9, 8], it is shown that linear forcing is a proper method for modeling forced MHD turbulence in physical space. Detailed information concerning linear forcing for compressible MHD turbulence one can find in [9]. The expressions of the external force, which allows obtaining a statistically stationary regime of turbulence, are derived. The formulas used for the formulation of large-eddy simulation approach are obtained. The potential possibilities of the LES method to reproduce physics of the flow under investigation in a stationary regime both for polytropic and for heat-conducting fluids are studied in detailed [9].

In Fig.10 and Fig.11 temporal evolution of kinetic energy and magnetic energy is presented for case of polytropic plasma. It is visible from the numerical results that statistically stationary turbulence arises after an initial time interval when large fluctuations are observed and the values of E_K and E_M practically do not vary with time. This means the balance between dissipation and energy injected in the system is occurred. It is interesting to note that E_K reaches a stationary regime slightly faster than E_M . The study of inertial range properties is one of the main tasks in studies of scale-similarity spectra of MHD turbulence. Inertial range properties are defined as time averages over periods of stationary turbulence conditions [18]. Kolmogorov-like spectrum $-5/3$ is observed when MHD turbulence is examined and magnetic energy is much less than kinetic energy, that is, nonlinear interactions are much more considerable than magnetic ones and the fluid is practically neutral hydrodynamic. In Fig.12, spectra of the kinetic and the magnetic energies are shown (solid line is the kinetic energy spectrum and dashed line is the magnetic energy spectrum). The spectra are normalized by factor $k^{5/3}$. Dot line represents Kolmogorov

scaling. The spectra of the kinetic and magnetic energy are obtained after time averaging of values in statistically stationary regime and there is clearly marked inertial turbulent range with the Kolmogorov-like spectrum $k^{-5/3}$ for both kinetic energy and magnetic energy as follows from Fig.12. The residual energy spectrum [19] that is determined as $E_R^K = |E_M^K - E_K^K|$ was studied in [9]. This spectrum is of interest because it gives an insight into the spectral interplay of kinetic and magnetic energies and exhibits self-similar scaling. It is demonstrated the normalized smoothed spectrum of residual energy and $E_R^K \sim k^{-7/3}$ in inertial range of turbulence which was theoretically obtained and was numerically confirmed for incompressible MHD turbulence [19]. It is apparent that there are no differences observed in statistical properties in inertial range due to weak compressibility (such result has been obtained recently for compressible hydrodynamic turbulence of neutral gas [20]). Accordingly, the proposed linear forces in LES provide correct results in studies of MHD turbulence.

It is shown in [9] that for the case when the kinetic energy of the flow is initially much larger than the magnetic energy, a Kolmogorov-like spectrum is obtained. When the magnetic energy is initially larger than the kinetic energy, the Iroshnikov-Kraichnan spectrum occurs. Thus, we have demonstrated the efficiency of the LES method for studies of scale-invariant properties of compressible MHD turbulence. The linear representation of the driving force developed for the LES method may also be of use in the DNS approach.

The obtained results can be used to study turbulent flows in various problems of space and astrophysical plasmas, in thermonuclear plasmas, plasma aerodynamics and problems in engineering applications. Thus, LES method has good future trends for research of compressible magnetohydrodynamic turbulence.

Acknowledgments

The work was supported by the program P-22 of Russian Academy of Science Presidium "Basic problems in solar system studies", Russian Foundation for Basic Research (13-05-90436, 14-02-31848) and Grant of President of Russian Federation for supporting young Russian scientists (MK-267.2014.5).

References

- [1] Chernyshov A A, Karelsky K V and Petrosyan A S 2006 *Phys. Plasmas* **13** 032304
- [2] Chernyshov A A, Karelsky K V and Petrosyan A S 2006 *Phys. Plasmas* **13** 104501
- [3] Chernyshov A A, Karelsky K V and Petrosyan A S 2008 *Physics of Fluids* **20** 085106
- [4] Chernyshov A A, Karelsky K V and Petrosyan A S 2007 *Physics of Fluids* **19** 055106
- [5] Chernyshov A A, Karelsky K V and Petrosyan A S 2008 *Flow, Turbulence and Combustion* **80** 21–35
- [6] Chernyshov A A, Karelsky K V and Petrosyan A S 2008 *Astrophysical Journal* **686** 1137–1144
- [7] Chernyshov A A, Karelsky K V and Petrosyan A S 2009 *Theor. Comput. Fluid Dyn.* **23** 451–470
- [8] Chernyshov A A, Karelsky K V and Petrosyan A S 2012 *Flow, Turbulence and Combustion* **89** 563–587
- [9] Chernyshov A A, Karelsky K V and Petrosyan A S 2010 *Phys. Plasmas* **17** 102307
- [10] Biskamp D 2003 *Magnetohydrodynamic turbulence* (United Kingdom: Cambridge University Press)
- [11] Ferziger J 1996 *Simulation and Modeling of Turbulent Flows* ed Gatski T, Hussami Y and Lumley J (Oxford University Press, New York (NY)) pp 109–154
- [12] Bardina J, Ferziger J H and Reynolds W C 1980 *AIAA 13th Fluid and Plasma Dynamics Conference, Snowmass, Colo* p 10
- [13] Germano M, Piomelli U, Moin P and Cabot W 1991 *Phys. Fluids A* **3** 1760–1765
- [14] Germano M 1992 *J. Fluid. Mech.* **238** 325–336
- [15] Müller W C and Carati D 2002 *Phys. Plasmas* **9** 824–834
- [16] Lilly D 1992 *Phys. Fluids A* **4** 633–635
- [17] Low M M M, Klessen R S, Burkert A and Smith M D 1998 *Phys. Rev. Lett.* **80** 2754–2764
- [18] Biskamp D and Müller W 2000 *Physics of Plasmas* **7** 4889–4900
- [19] Müller W C and Grappin R 2004 *Plasma Phys. Control. Fusion* **45** B91B96
- [20] Benzi R, Biferale L, Fisher R T, Kadanoff L P, Lamb D Q and Toschi F 2008 *Physical Review Letters* **100** 234503–+